Proceedings of ALGORITMY 2020
pp. 71–80

ON FINITE ELEMENT APPROXIMATION OF INCOMPRESSIBLE FLUID FLOW IN COMPUTATIONAL DOMAIN WITH VIBRATING WALLS: MATHEMATICAL MODELS FOR TREATMENT OF CHANNEL CLOSING *

PETR SVÁČEK†

Abstract. In this paper a simplified mathematical model of a voice production problem is considered. Here we focus on modelling of the glottis closure, which is an important part of phonation process. A simplified vocal fold model describing the vocal fold vibrations with two degrees of freedom is considered and coupled with a simplified model of the fluid flow described by the incompressible Navier-Stokes equations. The vocal fold vibrations cause a deformation of the fluid computational domain which is treated with the aid the Arbitrary Lagrangian-Eulerian method. The vibrations can possible lead to an appearance of the vocal folds contact. This situation is treated with the aid of a combination of inlet boundary conditions, a fictitious porous media approach and the Hertz impact forces. Numerical method is based on the stabilized finite element method. Numerical results are presented.

Key words. aeroelasticity, finite element method, contact problem

AMS subject classifications. 65N30, 76D05, 76Q05, 74M20

1. Introduction.

Human phonation process is a complex phenomena consisting of the air flow, structural vibrations, their mutual interactions and periodical appearing of the vocal folds contacts, see [6]. Except this also the acoustics phenomena is important. One important aspect is that the phonation is in fact an aeroelastic instability. This aeroelastic instability causes vocal folds oscillations with large amplitudes leading to their mutual contact. This periodical contact leads to the closure of the vocal tract at glottal part. Thus a realistic mathematical model should consist of the fluid-structure interaction description as well as a mathematical model of the (periodical) contact of the vocal folds. As such a treatment is extremely difficult, usually a simplified models are employed, see e.g. the simplified two degrees of freedom model of the vocal folds of [3] or the aeroelastic model in [2].

This paper presents a complex mathematical model consisting of the fluid flow problem, the structural description by motion equations, coupling conditions and a treatment of the contact problem. For the fluid flow the model of incompressible Navier-Stokes equations is used written in the arbitrary Lagrangian-Eulerian(ALE) form. The acoustic modelling is omitted in this paper as the influence of acoustic forces on the fluid flow or on the structure motion is negligible in the voice production process.

Further, the numerical approximation based on the finite element(FE) method is described, where the attention is paid step by step to the time discretization, weak formulation, stabilization of the FE method, linearization and to the solution of the linearized problem. The described approach is applied for solution of a benchmark problem.

*The financial support was provided by the *Czech Science Foundation* under the *Grant No. 19 - 07744S*

†Department of Technical Mathematics, Faculty of Mechanical Engineering, Czech Technical University in Prague, Karlovo nám. 13, 121 35 Praha 2, Czech Republic

2. Mathematical model.

2.1. Flow problem. The air flow in terms of the flow velocity $\boldsymbol{u} = (u_1, u_2)$ and the kinematic pressure p is modelled by the system of the Navier-Stokes equations (cf. [1]) written in the ALE form (cf. [4]), i.e. in the computational domain Ω_t it is governed by

$$\frac{D^{\mathcal{A}}\boldsymbol{u}}{Dt} + ((\boldsymbol{u} - \boldsymbol{w}_D) \cdot \nabla)\boldsymbol{u} = \operatorname{div} \boldsymbol{\tau}^f, \tag{2.1}$$
$$\nabla \cdot \boldsymbol{u} = 0,$$

where $\boldsymbol{\tau}^f = (\tau^f_{ij})$ is the fluid stress tensor given by $\boldsymbol{\tau}^f = -p\mathbb{I} + 2\nu\boldsymbol{D}$, $\boldsymbol{D}$ is the symmetric gradient tensor $\boldsymbol{D}(\boldsymbol{u}) = \frac{1}{2}(\nabla\boldsymbol{u} + \nabla^T\boldsymbol{u})$ with components $d_{ij} = \frac{1}{2}(\frac{\partial u_i}{\partial x_j} + \frac{\partial u_j}{\partial x_i})$ and $\nu > 0$ is the constant kinematic fluid viscosity. In Equations (2.1) $\boldsymbol{w}_D$ denotes the domain velocity and $\frac{D^{\mathcal{A}}\boldsymbol{u}}{Dt}$ is the ALE derivative, i.e. the derivative with respect to the reference configuration Ω_{ref}, cf. [4].

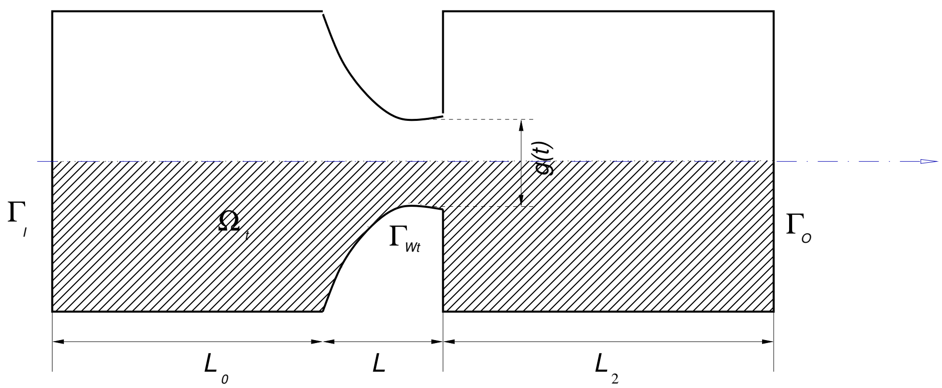

FIG. 2.1. *The computational domain Ω_t with specification of the boundary parts.*

In order to solve system (2.1) an initial and mixed boundary conditions are prescribed at the boundary $\partial\Omega_t$ of the computational domain. To this end it is assumed $\partial\Omega_t$ is at any time $t \in [0, T]$ formed by mutually disjoint parts $\partial\Omega_t = \Gamma_I \cup \Gamma_S \cup \Gamma_O \cup \Gamma_t$. Here, Γ_I denotes the inlet part of the boundary, Γ_O is the outlet part of the boundary, Γ_S denotes the axis of symmetry (in this paper it is part of x-axis $y = 0$ with the unit outward normal $\boldsymbol{n} = (0, 1)$) and $\Gamma_t = \Gamma_{Wt} \cup \Gamma_{Wf}$ denotes either the fixed (Γ_{Wf}) or the deformable (Γ_{Wt}) walls. The following boundary conditions are prescribed

$$\begin{aligned}
&\text{a) } \boldsymbol{u} = \boldsymbol{w}_D \text{ on } \Gamma_{Wt},\\
&\text{b) } u_2 = 0, -\tau_{12} = 0 \text{ on } \Gamma_S,\\
&\text{c) } \frac{1}{2}(\boldsymbol{u} \cdot \boldsymbol{n})^- \boldsymbol{u} - \boldsymbol{n} \cdot \boldsymbol{\tau} = \frac{1}{\varepsilon}(\boldsymbol{u} - \boldsymbol{u}_I) \text{ on } \Gamma_I,\\
&\text{d) } \frac{1}{2}(\boldsymbol{u} \cdot \boldsymbol{n})^- \boldsymbol{u} - \boldsymbol{n} \cdot \boldsymbol{\tau} = p_{ref}\boldsymbol{n} \text{ on } \Gamma_O,
\end{aligned} \tag{2.2}$$

where $\boldsymbol{n}$ denotes the unit outward normal vector to $\partial\Omega_t$, $\boldsymbol{u}_I$ is a prescribed inlet velocity, p_{ref} is a reference pressure value ($p_{ref} = 0$ in what follows), $\varepsilon > 0$ is a penalization parameter and α^- denotes the negative part of a real number α. Here, the boundary condition (2.2c) weakly imposes the Dirichlet boundary condition $\boldsymbol{u} = \boldsymbol{u}_I$ with the aid of a penalization parameter ε.

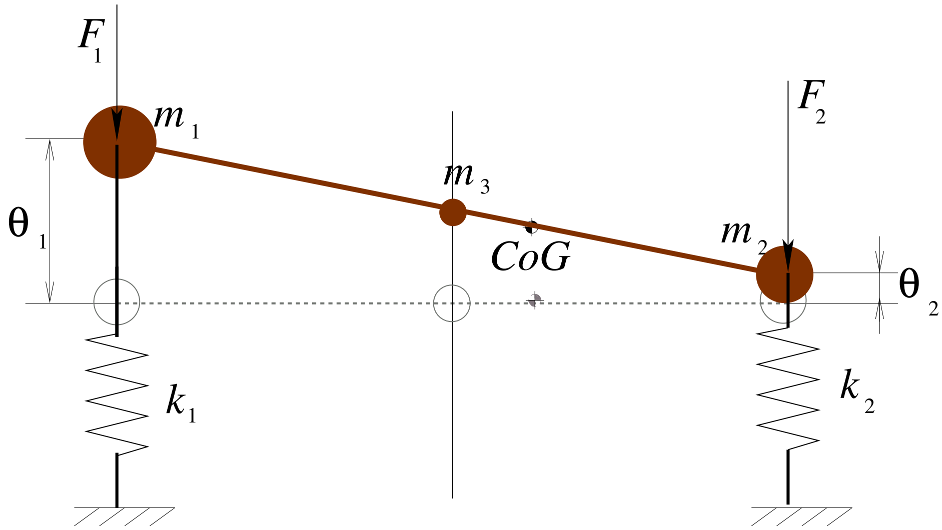

FIG. 2.2. *Two degrees of freedom model (with masses m_1, m_2, m_3) in displaced position (displacements θ_1 and θ_2) The acting aerodynamic forces F_1 and F_2 are shown.*

2.2. Structure model. A simplified structural model of the vocal fold is used modelled as a rigid body consisting of three masses (m_1, m_2 and m_3), see Fig. 2.1. The vocal fold motion is governed by the displacements $\theta_1(t)$ and $\theta_2(t)$ of the two masses m_1 and m_2. The equation of motion (see [2] for details) reads

$$\mathbb{M}\ddot{\boldsymbol{\theta}} + \mathbb{B}\dot{\boldsymbol{\theta}} + \mathbb{K}\boldsymbol{\theta} = -\boldsymbol{F}, \tag{2.3}$$

where $\boldsymbol{\theta} = (\theta_1, \theta_2)^T$, $\mathbb{M}$ is the mass matrix of the system, $\mathbb{K} = \mathrm{diag}(k_1, k_2)$ is the diagonal stiffness matrix of the system characterized by spring constants k_1, k_2, and $\mathbb{B} = \varepsilon_1\mathbb{M} + \varepsilon_2\mathbb{K}$ is the matrix of the proportional structural damping, ε_1, ε_2 are the constants of the proportional damping. The mass matrix is given by

$$\mathbb{M} = \begin{pmatrix} m_1 + \frac{m_3}{4} & \frac{m_3}{4} \\ \frac{m_3}{4} & m_2 + \frac{m_3}{4} \end{pmatrix}. \tag{2.4}$$

The vector $\boldsymbol{F} = \boldsymbol{F}_{imp} + \boldsymbol{F}_{aero}$ consists of the aerodynamical forces $\boldsymbol{F}_{aero} = (F_1, F_2)^T$ and the Herz impact forces $\boldsymbol{F}_{imp}$ due to the possible impact of vocal folds.

2.3. Coupling conditions. The aerodynamical forces F_1, F_2 are evaluated with the aid of the aerodynamical lift force $L(t)$ and aerodynamical torsional moment $M(t)$ acting on the surface of the structure Γ_{Wt}. The aerodynamical lift force and the aerodynamical torsional moment are evaluated with the aid of the mean (kinematic) pressure p and the mean flow velocity $\boldsymbol{u} = (u_1, u_2)$ as the integrals over the surface of the airfoil

$$L = -l\int_{\Gamma_{Wt}} \rho\tau_{2j}n_j\,dS, \quad M = l\int_{\Gamma_{Wt}} \rho\tau_{ij}n_j r_i^{\mathrm{ort}}\,dS, \tag{2.5}$$

where l denotes the depth of the profile section, and the vector r^{ort} has components $r_1^{\mathrm{ort}} = -(x_2 - x_2^{\mathrm{EA}})$, $r_2^{\mathrm{ort}} = x_1 - x_1^{\mathrm{EA}}$ with $(x_1^{\mathrm{EA}}, x_2^{\mathrm{EA}})$ being the position of the structure elastic axis.

The displacement of any point $\boldsymbol{\xi} = (\xi_1, \xi_2) \in \Gamma_{Wt}$ is determined in terms of θ_1, θ_2 as $\mathcal{A}_t(\boldsymbol{\xi}) = (\xi_1, y)$, where

$$y = \xi_2 + \frac{\theta_1 + \theta_2}{2} + (\xi_2 - \frac{L_{ref}}{2})(\theta_2 - \theta_1). \tag{2.6}$$

This displacement is used as boundary condition for the sought ALE mapping $\mathcal{A}_t$, which maps the reference domain Ω_0^{ref} onto the computational domain Ω_t. Consequently the domain velocity at the surface Γ_{Wt} is determined by θ_1, θ_2, whereas the domain velocity in the interior of the domain Ω_t needs to be evaluated as the time derivative of the ALE mapping $\mathcal{A}_t$.

2.4. Treatment of the contact. The use of the simplified structural model in combination with the symmetry assumption allows to calculate the gap $g(t)$ between the vocal folds in terms of the initial gap $g(0)$ and the values of displacements $\theta_1(t)$ and $\theta_2(t)$, see Figure 2.1. Let us emphasize that the solution of the ordinary differential equations (2.3) formally allows this gap become zero or even negative - this situation corresponds to the impact of the vocal folds. On the other hand the displacement of the part Γ_{Wt} based on the displacements $\theta_1(t)$ and $\theta_2(t)$ (as part of the computational domain) is both geometrically not possible as well as physically incorrect (as during the impact the surface of the vocal fold is deformed at the contact area) for the case of $g(t)$ being negative.

Moreover for the computational purposes (to avoid mesh distortion) it is also difficult to treat values of $g(t)$ being still positive but close to zero. Consequently the deformation of Γ_{Wt} is treated with the aid of the formula (2.6) for the gap $g(t) \geq g_{min} > 0$ (here g_{min} is usually specified as a small fraction of the initial gap). Two modifications of this formula are considered in the case when $g(t)$ becomes lower then g_{min}.

The first approach is a simple vertical shift of the (rigid) vocal fold which keeps the actual (fictitious) gap $g(t)$ equal to g_{min}. This means that the equation (2.6) is replaced by

$$y = \xi_2 + \frac{\theta_1 + \theta_2}{2} - (g_{min} - g(t))^+ + (\xi_2 - \frac{L_{ref}}{2})(\theta_2 - \theta_1). \tag{2.7}$$

where $(g_{min} - g(t))^+$ denotes the positive part of the number $g_{min} - g(t)$, i.e. it is either zero if $g(t) \geq g_{min}$ or it shifts the whole surface to keep the the gap equal g_{min} otherwise.

The second more realistic approach is based on a modification of the displacement of only the points in the contact zone. This is realized by modification of Equation (2.6) for mesh vertices which violate the condition of $g(t) \geq g_{min}$, i.e. Equation (2.6) is modified as

$$y = \min(\tilde{y}, g_{min}) \tag{2.8}$$

where $\tilde{y}$ is computed by the original formula (2.6)

$$\tilde{y} = \xi_2 + \frac{\theta_1 + \theta_2}{2} + (\xi_2 - \frac{L_{ref}}{2})(\theta_2 - \theta_1). \tag{2.9}$$

In both cases the computational fluid domain Ω_t is formally decomposed into two parts, $\Omega_t = \Omega_t^P \cup \Omega_t^f$ where by Ω_t^f the domain occupied by fluid is denoted and by Ω_t^P the part of the computational domain which should be occupied by the vocal tract (with no fluid) is denoted. The flow through the domain Ω_t^p is modelled as flow through a fictitious porous media, see Fig. 2.3, i.e. the Navier-Stokes equations are modified by an added Darcy term $\sigma_P \boldsymbol{u}$ in Ω_t^P

$$\frac{D^{\mathcal{A}}\boldsymbol{u}}{Dt} + ((\boldsymbol{u} - \boldsymbol{w}_D)\cdot\nabla)\boldsymbol{u} + \sigma_P \boldsymbol{u} = \operatorname{div} \boldsymbol{\tau}^f. \tag{2.10}$$

In practical realization Equation (2.10) is solved in the whole domain Ω_t with $\sigma_P = 0$ in Ω_t^f and with a suitable chosen constant $\sigma_P > 0$ in Ω_t^P.

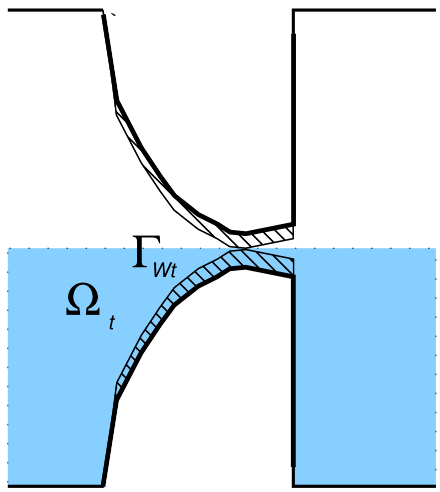

FIG. 2.3. *The detail of the porous media flow domain Ω_t^p.*

3. Numerical approximation. The numerical discretization of the described coupled problem is realized by the stabilized finite element method applied for approximation of the fluid part, solution of the motion equations with the aid of 4th order Runge-Kutta method and coupling of both parts with the aid of a strongly coupled algorithm. For the purpose of the time discretization the time interval I is divided by an equidistant partition $t_j = j\Delta t$ with a constant time step $\Delta t > 0$. The approximations of velocity and pressure at time instant t_j are denoted by $\boldsymbol{u}^j \approx \boldsymbol{u}(\cdot, t_j)$ and $p^j \approx p(\cdot, t_j)$ for $j = 0, 1, \ldots$. Similarly, by $\boldsymbol{w}_D^j$ and Ω^j approximations of the domain velocity $\boldsymbol{w}_D(\cdot, t_j)$ and the computational domain Ω_{t_j} at time instant t_j are denoted. In what follows we focus on numerical discretization at a (fixed) time step t_{n+1}. For the sake of simplicity the indices $n+1$ are omitted in what follows, i.e. the following notation is used $\boldsymbol{u} := \boldsymbol{u}^{n+1}$, $p := p^{n+1}$, $\boldsymbol{w}_D := \boldsymbol{w}_D^{n+1}$ and $\Omega := \Omega^{n+1}$.

3.1. Flow problem. In order to discretize equations (2.1) we start with approximation of the ALE time derivative at $t = t_{n+1}$ by the second order backward difference formula

$$\frac{D^{\mathcal{A}}\boldsymbol{u}}{Dt}\Big|_{t_{n+1}} \approx \frac{3\boldsymbol{u}^{n+1} - 4\tilde{\boldsymbol{u}}^n + \tilde{\boldsymbol{u}}^{n-1}}{2\Delta t} \tag{3.1}$$

where at a given time instant $t = t_{n+1}$ the velocity $\boldsymbol{u}^k$ defined on Ω^k is transformed to the velocity field $\tilde{\boldsymbol{u}}^k$ defined on $\Omega = \Omega^{n+1}$ by

$$\tilde{\boldsymbol{u}}^k(x) = \boldsymbol{u}^k(\mathcal{A}_{t_k}(\mathcal{A}_{t_{n+1}}^{-1}(x))), \quad x \in \Omega. \tag{3.2}$$

Further, the finite element discretization is based on the weak reformulation of time discretized equations (2.1). The function spaces for velocity and pressure are defined as $\boldsymbol{\mathcal{V}}$ and $\mathcal{Q}$ given by

$$\boldsymbol{\mathcal{V}} = \{\boldsymbol{\varphi} \in \boldsymbol{H}^1(\Omega) : \ \boldsymbol{\varphi} \cdot \boldsymbol{n} = 0 \text{ at } \Gamma_S\}, \qquad \mathcal{Q} = L_2(\Omega). \tag{3.3}$$

The space $\boldsymbol{\mathcal{X}}$ of test functions is subspace of $\boldsymbol{\mathcal{V}}$ specified as

$$\boldsymbol{\mathcal{X}} = \{\boldsymbol{\varphi} \in \boldsymbol{H}^1(\Omega) : \ \boldsymbol{\varphi} = 0 \text{ at } \Gamma_{W_t}, \ \boldsymbol{\varphi} \cdot \boldsymbol{n} = 0 \text{ at } \Gamma_S\}. \tag{3.4}$$

The weak form of Equations (2.1) is derived in the standard form: first, the ALE time derivative is replaced using the formula (3.1), next the first equation of (2.1) is multiplied by a test function $\boldsymbol{z} \in \boldsymbol{\mathcal{X}}$, integrated over Ω, the Green's theorem for viscous terms and the pressure gradient is used and the boundary conditions (2.2) as well as the definition of spaces $\boldsymbol{\mathcal{V}}$, $\boldsymbol{\mathcal{X}}$ are taken into an account. Similarly the second equation is multiplied by a test function $q \in \mathcal{Q}$, integrated over Ω and both equations are summed up together.

Thus we arrive to the weak form: Find $U = (\boldsymbol{u}, p) := (\boldsymbol{u}^{n+1}, p^{n+1}) \in \boldsymbol{\mathcal{V}} \times \mathcal{Q}$ such that $\boldsymbol{u}$ satisfy the boundary condition (2.2a) and

$$a(U; U, V) = L(V) \tag{3.5}$$

holds for any $V = (\boldsymbol{z}, q) \in \mathcal{X} \times \mathcal{Q}$. The forms a and L are defined for any $U = (\boldsymbol{u}, p) \in \boldsymbol{\mathcal{V}} \times \mathcal{Q}$, $\overline{U} = (\overline{\boldsymbol{u}}, \overline{p}) \in \boldsymbol{\mathcal{V}} \times \mathcal{Q}$ and $V = (\boldsymbol{z}, q) \in \boldsymbol{\mathcal{X}} \times \mathcal{Q}$ as follows

$$\begin{aligned} a(\overline{U}; U, V) = {} & \left((\frac{3}{2\Delta t} + \sigma_P)\boldsymbol{u}, \boldsymbol{z} \right)_\Omega + c(\overline{U}; U, V) + (2\nu \boldsymbol{D}(\boldsymbol{u}), \boldsymbol{D}(\boldsymbol{z}))_\Omega + \\ & + \frac{1}{\varepsilon}(\boldsymbol{u}, \boldsymbol{z})_{\Gamma_I} + \left(\frac{1}{2}(\overline{\boldsymbol{u}} \cdot \boldsymbol{n})^+ \boldsymbol{u}, \boldsymbol{z} \right)_{\Gamma_I \cup \Gamma_O} + (\nabla \cdot \boldsymbol{u}, q)_\Omega - (\nabla \cdot \boldsymbol{z}, p)_\Omega \end{aligned} \tag{3.6}$$

and

$$L(V) = \left(\frac{4\tilde{\boldsymbol{u}}^n - \tilde{\boldsymbol{u}}^{n-1}}{2\Delta t}, \boldsymbol{z} \right)_\Omega + \frac{1}{\varepsilon}(\boldsymbol{u}_I, \boldsymbol{z})_{\Gamma_I} - \int_{\Gamma_O} p_{ref}(\boldsymbol{n} \cdot \boldsymbol{z}) dS, \tag{3.7}$$

where by the symbol $(\cdot, \cdot)_{\mathcal{M}}$ the dot product in $L_2(\mathcal{M})$ or $\boldsymbol{L}_2(\mathcal{M})$ is denoted. Further, the skew-symmetric trilinear form c represents the convection term (here we abbreviate $\overline{\boldsymbol{w}} = \overline{\boldsymbol{u}} - \boldsymbol{w}_D^{n+1}$)

$$c(\overline{U}; U, V) = \frac{1}{2}\left((\overline{\boldsymbol{w}} \cdot \nabla)\boldsymbol{u}, \boldsymbol{z}\right)_\Omega - \frac{1}{2}\left((\overline{\boldsymbol{w}} \cdot \nabla)\boldsymbol{z}, \boldsymbol{u}\right)_\Omega + \frac{1}{2}\left((\nabla \cdot \boldsymbol{w}_D^{n+1})\boldsymbol{u}, \boldsymbol{z}\right)_\Omega. \tag{3.8}$$

In order to approximate problem (3.5) by finite element method, the spaces $\boldsymbol{\mathcal{V}}$ and $\boldsymbol{\mathcal{X}}$ are approximated using their FE subspaces $\boldsymbol{\mathcal{V}}_h$ and $\boldsymbol{\mathcal{X}}_h$, respectively. These spaces are constructed over an admissible triangulation $\mathcal{T}_\Delta$ of the domain Ω. Similarly, the pressure space $\mathcal{Q}$ is approximated by its FE subspace $\mathcal{Q}_h$ constructed again over the same triangulation $\mathcal{T}_\Delta$. Here, the Taylor-Hood FEs are used, i.e. the spaces of continuous piecewise quadratic functions defined by

$$\boldsymbol{\mathcal{W}}_h = \{\boldsymbol{\varphi} \in \boldsymbol{C}(\overline{\Omega}) : \boldsymbol{\varphi} \in \boldsymbol{P}_2(K) \ \forall K \in \mathcal{T}_\Delta\}, \quad \boldsymbol{\mathcal{V}}_h = \boldsymbol{\mathcal{W}}_h \cap \boldsymbol{\mathcal{V}} \quad \boldsymbol{\mathcal{X}}_h = \boldsymbol{\mathcal{W}}_h \cap \boldsymbol{\mathcal{X}},$$

are used for velocities and the space of continuous piecewise linear functions

$$\mathcal{Q}_h = \{\varphi \in C(\overline{\Omega}) : \varphi \in P_1(K) \ \forall K \in \mathcal{T}_\Delta\}.$$

are used for pressure approximations.

The FE approximations of $\boldsymbol{u}_h \approx \boldsymbol{u}$ and $p_h \approx p$ are then sought in the FE spaces $\boldsymbol{\mathcal{V}}_h \times \mathcal{Q}_h$ constructed over an admissible triangulation τ_h of the computational domain Ω_t^f: Find an approximate solution $U_h = (\boldsymbol{u}_h, p_h) \in \boldsymbol{\mathcal{V}}_h \times \mathcal{Q}_h$ such that Eq. (3.5) holds for any test function $V_h = (\boldsymbol{z}_h, q_h) \in \boldsymbol{\mathcal{X}}_h \times \mathcal{Q}_h$. Instead of formulation (3.5) the stabilized finite element approximations $U_h = (\boldsymbol{u}_h, p_h)$ are sought in the space $\boldsymbol{\mathcal{V}}_h \times \mathcal{Q}_h$ such that

$$a(U_h; U_h, V_h) + \mathcal{P}(U_h, V_h) + \mathcal{S}(U_h; U_h, V_h) = L(V) + \mathcal{F}(U; V), \tag{3.9}$$

holds for any test function $V_h = (\boldsymbol{z}_h, q_h) \in \boldsymbol{\mathcal{X}}_h \times \mathcal{Q}_h$. Here, the stabilization terms $\mathcal{S}$, $\mathcal{F}$ and $\mathcal{P}$ represents the SUPG/PSPG stabilization terms and the div-div stabilization terms, respectively. These terms are defined for any $U_h = (\boldsymbol{u}_h, p_h) \in \boldsymbol{\mathcal{W}}_h \times \mathcal{Q}_h$, $\overline{U}_h = (\overline{\boldsymbol{u}}_h, \overline{p}_h) \in \boldsymbol{\mathcal{W}}_h \times \mathcal{Q}_h$ and $V_h = (\boldsymbol{z}_h, q_h) \in \boldsymbol{\mathcal{X}}_h \times \mathcal{Q}_h$

$$\begin{aligned}
\mathcal{S}(\overline{U}_h; U_h, V_h) &= \sum_{K \in \mathcal{T}_\Delta} \left((\frac{3}{2\Delta t} + \sigma_P)\boldsymbol{u}_h - \mu \triangle \boldsymbol{u}_h + (\overline{\boldsymbol{w}}_h \cdot \nabla)\, \boldsymbol{u}_h + \nabla p, \boldsymbol{\Psi}(V_h) \right)_K \\
\mathcal{F}(\overline{U}_h; V_h) &= \sum_{K \in \mathcal{T}_\Delta} \left(\frac{4\tilde{\boldsymbol{u}}_h^n - \tilde{\boldsymbol{u}}_h^{n-1}}{2\Delta t}, \boldsymbol{\Psi}(V_h) \right)_K \qquad (3.10) \\
\mathcal{P}(U_h, V_h) &= \sum_{K \in \mathcal{T}_\Delta} \tau_K \Big(\nabla \cdot \boldsymbol{u}_h, \nabla \cdot \boldsymbol{z}_h \Big)_K,
\end{aligned}$$

where $\boldsymbol{\Psi}(V_h) := \delta_K (\overline{\boldsymbol{w}}_h \cdot \nabla) \boldsymbol{z}_h + \delta_K \nabla q_h$, $\overline{\boldsymbol{w}}_h = \overline{\boldsymbol{u}}_h - \boldsymbol{w}_D^{n+1}$ and δ_K, τ_K are suitably chosen stabilization parameters.

The problem (3.9) is nonlinear and requires an iterative solution. Here, the approach based on the Oseen linearization is used. Starting with an approximation $U_h^0 \in \boldsymbol{\mathcal{V}}_h \times \mathcal{Q}_h$ the linearized problems are solved for $k = 0, 1, \ldots$: Find $U_h^{k+1} \in \boldsymbol{\mathcal{V}}_h \times \mathcal{Q}_h$ such that

$$a(U_h^k; U_h^{k+1}, V_h) + \mathcal{P}(U_h^k, V_h) + \mathcal{S}(U_h^k; U_h^{k+1}, V_h) = L(V_h) + \mathcal{F}(U_h^k; V_h), \tag{3.11}$$

holds for any $V_h \in \boldsymbol{\mathcal{X}}_h \times \mathcal{Q}_h$. This process is repeated till $\|U_h^{k+1} - U_h^k\| < \varepsilon$ with a suitable chosen $\varepsilon > 0$.

3.2. Structure model, ALE mapping and ALE derivative. The motion equations (2.3) are formulated as a first order system and time discretized with the aid of 4th order Runge-Kutta method. This method is used to find the approximations $\theta_1^n \approx \theta_1(t_n)$, $\theta_2^n \approx \theta_2(t_n)$, $\dot{\theta}_1^{\,n} \approx \dot{\theta}_1(t_n)$, $\dot{\theta}_2^{\,n} \approx \dot{\theta}_2(t_n)$ starting from an initial condition. Here, the zero initial condition is used $\theta_1^0 = \theta_2^0 = \dot{\theta}_1^{\,0} = \dot{\theta}_2^{\,0} = 0$ and the Runge-Kutta methods is applied on sub-intervals of the interval (t_n, t_{n+1}), where the aerodynamical forces F_1 and F_2 are interpolated in the interior of the interval from the values found at time instants t_n and t_{n+1}.

Based on the found displacements θ_1^{n+1}, θ_2^{n+1} at the time instant t_{n+1} the displacement of the boundary $\Gamma_{W t_{n+1}}$ is determined by equation (2.6). The ALE mapping $\mathcal{A}$ at time instant t_{n+1} is determined in terms of sought displacement of the reference domain with the Dirichlet boundary conditions specified by (2.6) at Γ_{Wref} and with the zero Dirichlet boundary condition otherwise. To this end the approach based on solution of a fictitious elastic problem is used similarly as in [7]. This approach however is strongly modified in order to keep the quality of the mesh satisfactory even in the case of almost enclosed channel. This is why, instead of solving of a linear elasticity problem, the geometrical non-linearities are taken into an account.

Once the ALE mapping at $\mathcal{A}_{t_{n+1}}$ is determined, the ALE domain velocity $\boldsymbol{w}_D^{n+1}$ is computed with the aid of the second order backward difference formula, i.e. for $x \in \Omega^{n+1}$ with a reference $\xi \in \Omega_{ref}$, we have

$$\boldsymbol{w}_D^{n+1}(x) \approx \frac{3x - 4x^n + x^{n+1}}{2\tau} \tag{3.12}$$

where $x = \mathcal{A}_{t_{n+1}}(\xi)$, $x^n = \mathcal{A}_{t_n}(\xi)$, $x^{n-1} = \mathcal{A}_{t_{n-1}}(\xi)$.

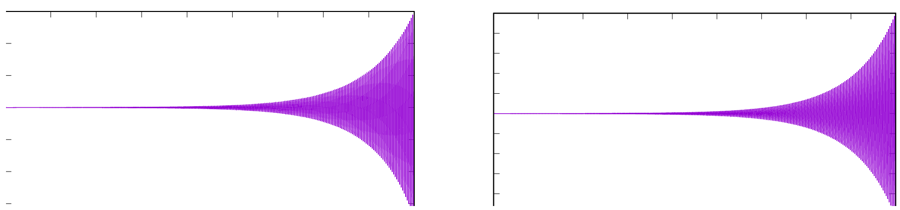

FIG. 4.1. *The aeroelastic responses $\theta_1(t)$ (left) and $\theta_2(t)$ (right) of the structure for flow velocity $U_\infty = 0.65$ m/s. The phonation onset phase is shown.*

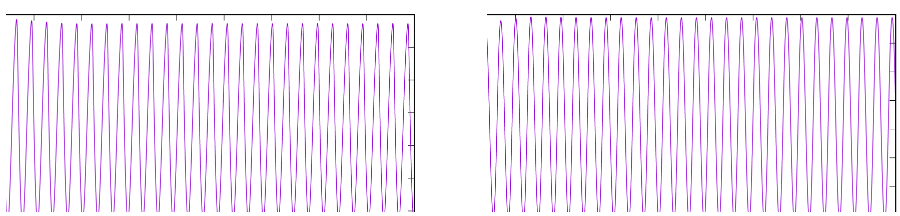

FIG. 4.2. *The aeroelastic response of the structure for flow velocity $U_\infty = 0.65$ m/s. The phonation phase with periodical closing of the gap between vocal folds and the Hertz impact forces involved.*

4. Numerical results. In this section benchmark the problem from [5] is numerically approximated by the proposed method using both approaches for treatment of the channel closing. For the inflow velocity $U_\infty = 0.65 m/s$ the aeroelastic instability occurred are shown in terms of the displacements θ_1 and θ_2 in Figure 4.1. In the context of the voice production this corresponds to the phonation onset. With further continuation the amplitude vibrations increases, but the limitation by the gap guarantees these vibrations to stay limited, and leads to a limit cycle of oscillations as shown in Figure-4.2. Here, the vibrating vocal folds starts influenced by their mutual contact. Figure 4.3 shows the vibrations in terms of the gap between the vocal folds. One can see that for the phonation onset the contact problem is unimportant (Figure 4.3, left), whereas during the phonation the gap between two vocal folds periodically becomes zero (Figure 4.3, right). This behaviour well corresponds to the results of simplified models. For a higher inflow velocity $U_\infty = 0.7 m/s$ similar behaviour was observed with much faster appearance of the phonation, see Fig. 4.4 and Fig. 4.5. Figures 4.6-4.7 then compares the two suggested approaches of geometrical gap closing in terms of flow velocity in the glottis region.

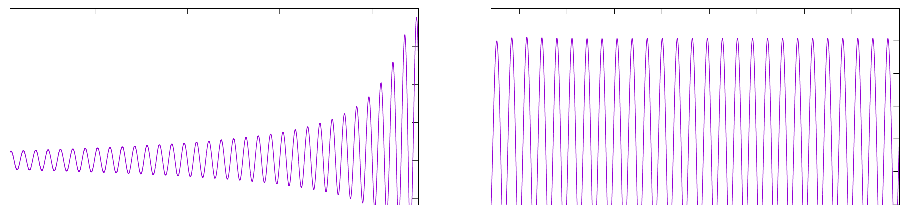

FIG. 4.3. *The aeroelastic response of the structure for flow velocity $U_\infty = 0.65$ m/s in terms of the gap $g(t)$.*

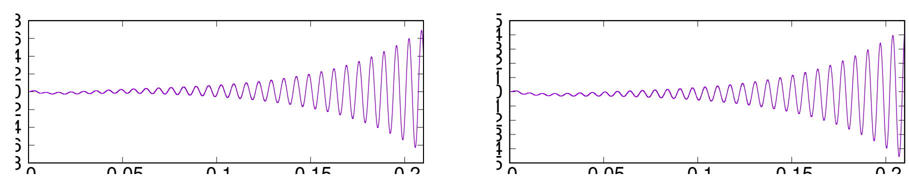

FIG. 4.4. *The aeroelastic responses $\theta_1(t)$ (left) and $\theta_2(t)$ (right) of the structure for flow velocity $U_\infty = 0.70$ m/s - phonation onset*

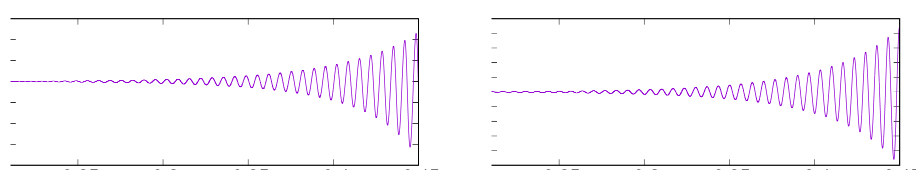

FIG. 4.5. *The aeroelastic responses $\theta_1(t)$ (left) and $\theta_2(t)$ (right) of the structure for flow velocity $U_\infty = 0.70$ m/s. The phonation onset phase is shown with much faster growth of the amplitudes.*

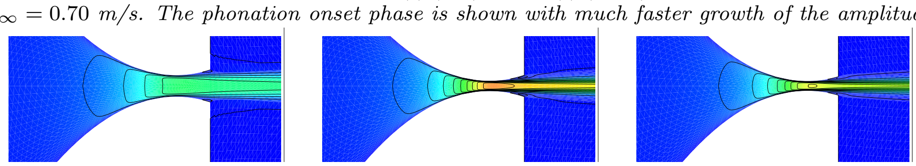

FIG. 4.6. *The flow velocity magnitude during the opening and closing phase for the inlet flow velocity $U_\infty = 0.65$ m/s, simple rigid body approach of closing applied*

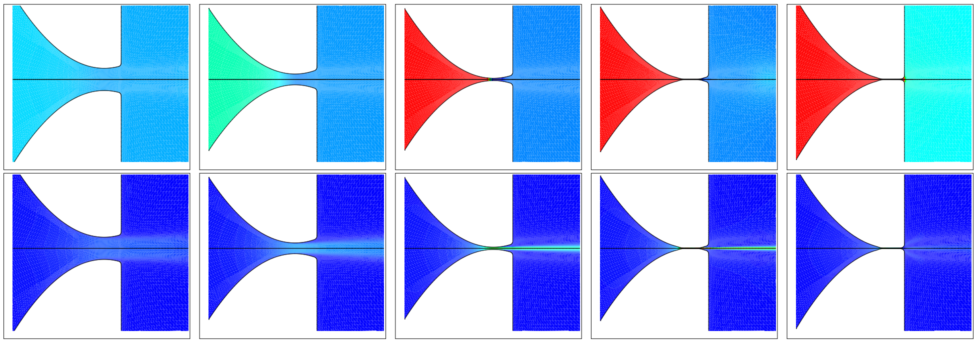

FIG. 4.7. *The flow velocity magnitude during the opening and closing phase for the inlet flow velocity* $U_\infty = 0.65$ *m/s - second approach*

5. Conclusion. This paper presents the detailed description of the numerical approximation of the problem of fluid-structure interaction problem used in models of human phonation. Main attention is paid to modelling of the contact of vibrating vocal folds. Here two strategies are suggested and numerical results are shown.

REFERENCES

[1] M. Feistauer. *Mathematical Methods in Fluid Dynamics.* Longman Scientific & Technical, Harlow, 1993.

[2] J. Horáček, P. Šidlof, and J. G. Švec. Numerical simulation of self-oscillations of human vocal folds with Hertz model of impact forces. *Journal of Fluids and Structures*, 20(6):853–869, 2005.

[3] K. Ishizaka and J. L. Flanagan. Synthesis of voiced sounds from a two-mass model of the vocal coords. *The Bell System Technical Journal*, 51:1233–1268, 1972.

[4] T. Nomura and T. J. R. Hughes. An arbitrary Lagrangian-Eulerian finite element method for interaction of fluid and a rigid body. *Computer Methods in Applied Mechanics and Engineering*, 95:115–138, 1992.

[5] P. Sváček and J. Horáček. Numerical simulation of glottal flow in interaction with self oscillating vocal folds: comparison of finite element approximation with a simplified model. *Communications in Computational Physics*, 12(3):789–806, 2012.

[6] I. R. Titze. *The Myoelastic Aerodynamic Theory of Phonation.* National Center for Voice and Speech, U.S.A., 2006.

[7] Z. Yang and D. J. Mavriplis. Unstructured dynamic meshes with higher-order time integration schemes for the unsteady Navier-Stokes equations. In *43rd AIAA Aerospace Sciences Meeting*, page 13 pp., Reno NV, January 2005. AIAA Paper 2005-1222.